Hindawi
Complexity
Volume 2019, Article ID 7941302, 13 pages
https://doi.org/10.1155/2019/7941302

Research Article

Nonlinear Backstepping Control Design for Coupled Nonlinear Systems under External Disturbances

Wonhee Kim[1], **Chang Mook Kang**[2], **Young Seop Son**[3] **and Chung Choo Chung**[4]

[1] *School of Energy Systems Engineering, Chung-Ang University, Seoul 06974, Republic of Korea*
[2] *Agency for Defense Development, Daejeon, Republic of Korea*
[3] *Global R&D Center, CAMMSYS Corporation, Incheon 406-840, Republic of Korea*
[4] *Division of Electrical and Biomedical Engineering, Hanyang University, Seoul 133-791, Republic of Korea*

Correspondence should be addressed to Chang Mook Kang; mook@add.re.kr

Received 25 October 2018; Revised 3 January 2019; Accepted 17 January 2019; Published 7 February 2019

Academic Editor: Eric Campos-Canton

A nonlinear backstepping control is proposed for the coupled normal form of nonlinear systems. The proposed method is designed by combining the sliding-mode control and backstepping control with a disturbance observer (DOB). The key idea behind the proposed method is that the linear terms of state variables of the second subsystem are lumped into the virtual input in the first subsystem. A DOB is developed to estimate the external disturbances. Auxiliary state variables are used to avoid amplification of the measurement noise in the DOB. For output tracking and unmatched disturbance cancellation in the first subsystem, the desired virtual input is derived via the backstepping procedure. The actual input in the second subsystem is developed to guarantee the convergence of the virtual input to the desired virtual input by using a sliding-mode control. The stability of the closed-loop is verified by using the input-to-state stable (ISS) property. The performance of the proposed method is validated via numerical simulations and an application to a vehicle system based on CarSim platform.

1. Introduction

Control for nonlinear systems has attracted considerable attention, and, therefore, various control methods have been investigated for nonlinear systems. Control methods using the Lyapunov function were proposed for nonlinear systems [1–4]. Input-output linearization and feedback linearization were proposed to transform nonlinear systems to the normal form and to control the nonlinear systems [5, 6]. Sliding-mode control techniques were developed for nonlinear systems owing to the decoupling and invariance properties [7, 8]. Control algorithms based on the singular perturbation theory were developed for nonlinear systems involving fast and slow dynamics [9, 10]. Backstepping method is one of the breakthroughs for the control of nonlinear systems. This method is a recursive procedure using a Lyapunov function and a systematic design approach for special forms of the nonlinear systems (the strict feedback form or the normal form or both) [11]. It can guarantee global stability and improvement of tracking and transient performances. In the past decades, various backstepping methods were widely used to solve the control problems of nonlinear systems. A backstepping control method was developed to improve the force control performance for an electro-hydraulic actuator [12]. An adaptive control technique was implemented to the backstepping controller for unknown disturbance or parameters [13]. An adaptive backstepping sliding-mode controller was designed to improve the tracking performance in the sliding and presliding phases [14]. In [15], an output feedback nonlinear control was proposed for a hydraulic system with mismatched modeling uncertainties; in this control, an extended state observer (ESO) and a nonlinear robust controller are synthesized via the backstepping method. A recurrent fuzzy neural network backstepping control was proposed for the prescribed output tracking performance of nonlinear dynamic systems [16]. An adaptive robust control using ESO was developed for the DC motor control [17]. An ESO-based backstepping was proposed to improve the output-tracking performance with external disturbance using only output feedback [18]. Active disturbance rejection

adaptive control schemes were proposed for both parametric uncertainties and uncertain nonlinearities of the nonlinear systems [19, 20]. An observer-based backstepping control method using reduced lateral dynamics was developed for autonomous lane-keeping system [21].

Let us consider a class of nonlinear systems coupled with two normal form subsystems as follows:

$$\begin{aligned}
\dot{x}_1 &= x_2 \\
&\vdots \\
\dot{x}_{r-1} &= x_r \\
\dot{x}_r &= f_r(x_a) + \sum_{i=r+1}^{n} a_i x_i + d_1 \\
\dot{x}_{r+1} &= x_{r+2} \\
&\vdots \\
\dot{x}_{n-1} &= x_n \\
\dot{x}_n &= f_n(x) + g(x)\,u + d_2 \\
y &= x_1
\end{aligned} \tag{1}$$

where $x = [x_1, x_2, \ldots, x_n]^T = [x_a, x_b]^T \in \mathbb{R}^n$ is the state variable vector, $x_a = [x_1, x_2, \ldots, x_r]^T \in \mathbb{R}^r$, $x_b = [x_{r+1}, x_{r+2}, \ldots, x_n]^T \in \mathbb{R}^{n-r}$, $y = x_1$ denotes the output, a_n is nonzero constant, the input function $g(x)$ is always positive or negative for all $x(t)$, and $d_1(t)$ and $d_2(t)$ are disturbances. In this paper, this class of systems (1) is called the coupled normal form in nonlinear systems. This nonlinear system (1) is not in the general normal form because x_{r+1} cannot be regarded as the virtual input in x_r dynamics. Furthermore, the disturbance d_1 is in x_r dynamics. Thus, previous backstepping control methods cannot be used directly for tracking control of these systems. Several methods were presented to solve the control problem of nonlinear systems [22, 23]. In [22], two nonlinear control techniques using backstepping and sliding mode techniques were applied to an autonomous microhelicopter. Recently, a robust nonlinear control was developed for the synchronization control of cross-strict feedback hyperchaotic systems [23]. Unfortunately, because systems in [22, 23] have multi-inputs, these techniques cannot solve the control problems for the coupled normal form in a nonlinear system (1).

In this paper, we propose a nonlinear backstepping control for the coupled normal form of nonlinear systems. The proposed method combines a sliding mode technique and backstepping control with the disturbance observer (DOB). The key idea of the proposed method is that the terms $\sum_{i=r+1}^{n} a_i x_i$ are lumped into the virtual input in the first subsystem. A DOB is developed to estimate the external disturbances. Auxiliary state variables are used to avoid amplification of the measurement noise in the DOB. For output tracking and unmatched disturbance cancellation in the first subsystem, the desired virtual input is derived via the backstepping procedure. The actual input in the second subsystem is developed to guarantee the convergence of the virtual input to the desired virtual input by using a super twisting algorithm (STA). The stability of the closed-loop is proven by using the input-to-state stable (ISS) property. The performance of the proposed method is validated via numerical simulations and an application to a vehicle system based on CarSim platform.

2. Disturbance Observer Design

In this paper, we describe the situation that satisfies the following Assumptions 1 and 2.

Assumption 1. d_1, d_2 and their derivatives are also bounded.

In general, prior information about the derivative of the disturbances is unknown but bounded, at least locally [24]. The unknown constants $\dot{d}_{1_{\max}}$ and $\dot{d}_{2_{\max}}$ exist such that

$$\begin{aligned}
\left|\dot{d}_1\right| &\le \dot{d}_{1_{\max}} \\
\left|\dot{d}_2\right| &\le \dot{d}_{2_{\max}}.
\end{aligned} \tag{2}$$

Assumption 2. The polynomial $a_n s^{n-r-1} + a_{n-1} s^{n-r-2} + \ldots + a_{r+1}$ is Hurwitz.

Most real systems that are in the form of (1) satisfy Assumption 2. For example, the lateral dynamics of a vehicle with differential braking force input satisfy Assumption 2 [25]. Thus, this assumption is not strict for actual physical systems.

From (1), the disturbances, d_1 and d_2, can be rewritten as

$$\begin{aligned}
d_1 &= \dot{x}_r - f_r(x_a) - \sum_{i=r+1}^{n} a_i x_i \\
d_2 &= \dot{x}_n - f_n(x) - g(x)\,u.
\end{aligned} \tag{3}$$

We define the estimations of the disturbances, $\hat{d}_1$ and $\hat{d}_2$. The dynamics of $\hat{d}_1$ and $\hat{d}_2$ are designed as

$$\begin{aligned}
\dot{\hat{d}}_1 &= \frac{1}{\varepsilon_1}\left(\dot{x}_r - f_r(x_a) - \sum_{i=r+1}^{n} a_i x_i - \hat{d}_1\right) \\
\dot{\hat{d}}_2 &= \frac{1}{\varepsilon_2}\left(\dot{x}_n - f_n(x) - g(x)\,u - \hat{d}_2\right)
\end{aligned} \tag{4}$$

where $1/\varepsilon_2$ and $1/\varepsilon_3$ are the observer gains. The estimation errors are defined as

$$\begin{aligned}
\tilde{d}_1 &= d_1 - \hat{d}_1 \\
\tilde{d}_2 &= d_2 - \hat{d}_2.
\end{aligned} \tag{5}$$

From, (3), (4), and (5), the estimation error dynamics can be derived as

$$\begin{aligned}\dot{\tilde{d}}_1 &= \dot{d}_1 - \dot{\hat{d}}_1 \\ &= \dot{d}_1 - \frac{1}{\varepsilon_1}\left(\dot{x}_r - f_r(x_a) - \sum_{i=r+1}^{n} a_i x_i - \hat{d}_1\right) \\ &= \dot{d}_1 - \frac{1}{\varepsilon_1}\left(d_1 - \hat{d}_1\right) = -\frac{1}{\varepsilon_1}\tilde{d}_1 + \dot{d}_1 \\ \dot{\tilde{d}}_2 &= \dot{d}_2 - \dot{\hat{d}}_2 = \dot{d}_2 - \frac{1}{\varepsilon_2}\left(\dot{x}_n - f_n(x) - g(x)u - \hat{d}_2\right) \\ &= \dot{d}_2 - \frac{1}{\varepsilon_2}\left(d_2 - \hat{d}_2\right) = -\frac{1}{\varepsilon_2}\tilde{d}_2 + \dot{d}_2.\end{aligned} \tag{6}$$

To suppress the bounded derivatives of the disturbances, the high gains, i.e., the low values of ε_1 and ε_2, are required. In practice, measurement noises do appear in sensors. The dynamics of $\hat{d}_1$ and $\hat{d}_2$ (4) employ the derivative of the state. If high observer gains are used, the noise is amplified by the high gains. Thus, the observer is not practical for implementation. To avoid the use of the derivative of the state, we use the auxiliary state variables, ξ_1, ξ_2.

Theorem 3. *With Assumption 1, given the auxiliary state variables, ξ_1, ξ_2 such as*

$$\begin{aligned}\xi_1 &= \hat{d}_1 - \frac{x_r}{\varepsilon_1} \\ \xi_2 &= \hat{d}_2 - \frac{x_n}{\varepsilon_2}\end{aligned} \tag{7}$$

the dynamics of the auxiliary state variables are

$$\begin{aligned}\dot{\xi}_1 &= -\frac{1}{\varepsilon_1}\left(\xi_1 + \frac{x_r}{\varepsilon_1}\right) + \frac{1}{\varepsilon_1}\left(-f_r(x_a) - \sum_{i=r+1}^{n} a_i x_i\right) \\ \dot{\xi}_2 &= -\frac{1}{\varepsilon_2}\left(\xi_2 + \frac{x_n}{\varepsilon_2}\right) + \frac{1}{\varepsilon_2}\left(-f_n(x) - g(x)u\right).\end{aligned} \tag{8}$$

Then, $|\tilde{d}_i(t)| \le \exp(-(1/2\varepsilon_i)t)|\tilde{d}_i(0)| + 2\varepsilon_i \dot{d}_{i_{\max}}$ for $i \in [1,2]$.

Proof. Differentiating the auxiliary state variables with respect to time gives

$$\dot{\xi}_i = \dot{\hat{d}}_i - \frac{\dot{x}_j}{\varepsilon_i} \tag{9}$$

for $i \in [1,2]$ and $j \in \{r, n\}$. From (1), (5), (7), and (8), the disturbance estimation error dynamics are obtained as

$$\dot{\tilde{d}}_i = -\frac{1}{\varepsilon_i}\tilde{d}_i + \dot{d}_i. \tag{10}$$

In (10), the dynamics of $\tilde{d}_i^2$ are

$$\begin{aligned}\frac{d}{dt}\left(\frac{\tilde{d}_i^2}{2}\right) &= -\frac{1}{\varepsilon_i}\tilde{d}_i^2 + \tilde{d}\dot{d}_i \\ &\le -\frac{1}{2\varepsilon_i}\tilde{d}_i^2 - \frac{1}{2\varepsilon_i}\left|\tilde{d}_i\right|\left(\left|\tilde{d}_i\right| - 2\varepsilon_i\left|\dot{d}_i\right|\right)\end{aligned} \tag{11}$$

The following result is thus derived from (11), using Lemma 6.20 and Theorem C.2 in [11]:

$$\begin{aligned}\left|\tilde{d}_i(t)\right| &\le \exp\left(-\frac{1}{2\varepsilon_i}t\right)\left|\tilde{d}_i(0)\right| + 2\varepsilon_i \sup_{0\le\tau\le t}\left|\dot{d}_i(\tau)\right| \\ &\le \exp\left(-\frac{1}{2\varepsilon_i}t\right)\left|\tilde{d}_i(0)\right| + 2\varepsilon_i \dot{d}_{i_{\max}}.\end{aligned} \tag{12}$$

The upper bound of $|\tilde{d}_i(\infty)|$ thus decreases as ε_i gets smaller. □

Remark 4. The proposed DOB (8) with the auxiliary state variable (7) does not require the derivatives of states, i.e., $\dot{x}_r$ and $\dot{x}_n$, to obtain $\dot{d}_1$ and $\dot{d}_2$. Thus, if (7) and (8) are used to estimate the disturbances instead of (4), amplification of the measurement noise by the high gain can be reduced, such that it is negligible in practice.

3. Sliding Mode Backstepping Controller Design

In this paper, the control goal is to determine u that makes the output $y = x_1$ track the desired reference trajectory $y_d = x_{1_d}$, which is assumed to have continuous derivatives up to the nth order. The tracking error e_i $i \in [1, r]$ is defined as

$$\begin{aligned}e_1 &= x_1 - y_d \\ e_2 &= \dot{x}_1 - \dot{y}_d \\ e_3 &= \ddot{x}_1 - \ddot{y}_d \\ &\vdots \\ e_r &= x_1^{(r-1)} - y_d^{(r-1)}.\end{aligned} \tag{13}$$

To eliminate the steady-state error, the integral error e_0 is defined as

$$e_0 = \int_0^t e_1(\tau)\, d\tau. \tag{14}$$

The error dynamics from e_1 to e_r can be written as

$$\begin{aligned}\dot{e}_0 &= e_1 \\ \dot{e}_1 &= e_2 \\ &\vdots \\ \dot{e}_{r-1} &= e_r \\ \dot{e}_r &= f_r(x_a) + \sum_{i=r+1}^{n} a_i x_i + d_1 - y_d^{(r)}.\end{aligned} \tag{15}$$

The linear combination of the tracking errors, s_1, is designed in terms of the error

$$s_1 = e_r + \sum_{i=0}^{r-1} \sigma_i e_i \tag{16}$$

where the coefficients $\sigma_0, \ldots, \sigma_{r-1}$ are chosen such that the polynomial $s^r + \sigma_{r-1}s^{r-1} + \cdots + \sigma_0$ is Hurwitz. From (15) and (16), we obtain $\dot{s}_1$ as

$$\dot{s}_1 = f_r(x_a) + \sum_{i=r+1}^{n} a_i x_i + d_1 - y_d^{(r)} + \sum_{i=0}^{r-1} \sigma_i e_{i+1}. \quad (17)$$

We define the terms, $\sum_{i=r+1}^{n} a_i x_i$, as the virtual input of the first subsystem in (1):

$$s_2 = \sum_{i=r+1}^{n} a_i x_i. \quad (18)$$

Equation (17) then becomes

$$\dot{s}_1 = f_r(x_a) + d_1 - y_d^{(r)} + \sum_{i=0}^{r-1} \sigma_i e_{i+1} + s_{2d} + z_2 \quad (19)$$

where s_{2d} is the desired virtual input and the sliding surface $z_2 = s_2 - s_{2d}$. The desired virtual input, s_{2d}, is designed as

$$s_{2d} = -f_r(x_a) - d_1 + y_d^{(r)} - \sum_{i=0}^{r-1} \sigma_i e_{i+1} - k_{s1} s_1 \quad (20)$$

where k_{s1} is positive and constant. The derivative of z_2 with respect to time is

$$\begin{aligned} \dot{z}_2 &= \dot{s}_2 - \dot{s}_{2d} = \sum_{i=r+1}^{n-1} a_i x_{i+1} + a_n \dot{x}_n - \dot{s}_{2d} \\ &= \sum_{i=r+1}^{n-1} a_i x_{i+1} + a_n \left(f_n(x) + g(x)u + d_2\right) - \dot{s}_{2d}. \end{aligned} \quad (21)$$

The input is designed using STA as

$$\begin{aligned} u = &-\frac{1}{a_n g(x)} \left(\sum_{i=r+1}^{n-1} a_i x_{i+1} - \dot{s}_{2d} + \phi_1(z_2) - \phi_2(z_2) \right) \\ &- \frac{1}{g(x)} \left(f_n(x) + d_2\right) \end{aligned} \quad (22)$$

where $\phi_1(z_2) = k_{z1}|z_2|^{1/2}\mathrm{sgn}(z_2)$, $\dot{\phi}_2(z_2) = -k_{z2}\,\mathrm{sgn}(z_2)$, and k_{z1} and k_{z2} are positive constants. In order to avoid the chattering problem, STA [26, 27] is applied to the controller (22).

Theorem 5. *With Assumption 2, suppose that the control law, (20) and (22), is applied to system (1). Then the output tracking error e_1 converges to zero and x_b is ultimately bounded.*

Proof.
Step 1. From (19) and (20), we have

$$\dot{s}_1 = -k_{s1} s_1 + z_2. \quad (23)$$

By defining the positive-definite Lyapunov function V_1 as

$$V_1 = \frac{1}{2} s_1^2 \quad (24)$$

we obtain

$$\dot{V}_1 = -k_{s1} s_1^2 + z_2 s_1. \quad (25)$$

Using z_2 as the input and s_1 as the output in (23) gives

$$\underbrace{z_2}_{input} \; \underbrace{s_1}_{output} = \dot{V}_1 + \underbrace{k_{s1} s_1^2}_{\geq 0}. \quad (26)$$

Then (26) shows that the relationship between s_1 and z_2 is strictly output passive [9] and $\dot{s}_1 = -k_{s1}s_1$ is zero-state observable. Therefore, s_1 system is ISS. With control law (22), the dynamics of z_2 and ϕ_2 become

$$\begin{aligned} \dot{z}_2 &= -k_{z1} |z_2|^{1/2} \mathrm{sgn}(z_2) + \phi_2 \\ \dot{\phi}_2 &= -k_{z2} \mathrm{sgn}(z_2). \end{aligned} \quad (27)$$

We define the vector $\zeta = [\zeta_1 \;\; \zeta_2]^T = [|z_2|^{1/2}\mathrm{sgn}(z_2), \;\; \phi_2]^T$. The derivative of ζ with respect to time is

$$\dot{\zeta} = \frac{1}{|\zeta_1|} A_\zeta \zeta \quad (28)$$

where

$$A_\zeta = \begin{bmatrix} -\frac{1}{2}k_{z1} & \frac{1}{2} \\ -k_{z2} & 0 \end{bmatrix} \quad (29)$$

and $|\zeta_1| = |z_2|^{1/2}$. Because $k_{z1} > 0$ and $k_{z2} > 0$, A_ζ is Hurwitz. We define the Lyapunov candidate function V_ζ as

$$V_\zeta = \zeta^T P_\zeta \zeta \quad (30)$$

where P_ζ is positive definite. The derivative of ζ with respect to time is given by

$$\dot{V}_\zeta = -\frac{1}{|\zeta_1|} \zeta^T Q_\zeta \zeta \quad (31)$$

where Q_ζ is positive definite such that $A_\zeta^T P_\zeta + P_\zeta A_\zeta = -Q_\zeta$. From [27], the origin $\zeta = 0$ is finite-time stable. Consequently z_2 is equal to zero, identically, after a finite time interval.

Step 2. With $z_2 = 0$,

$$\dot{s}_1 = -k_{s1} s_1. \quad (32)$$

Then, (16) can be rewritten as

$$\begin{aligned} \dot{e}_0 &= e_1 \\ &\vdots \\ \dot{e}_{r-1} &= e_r \\ e_r &= -\sum_{i=0}^{r-1} \sigma_i e_i + s_1. \end{aligned} \quad (33)$$

Equation (33) is simplified as

$$\dot{e}_a = A_a e_a + B_a s_1 \tag{34}$$

where $e_a = [e_0, e_1, \ldots, e_{r-1}]^T \in \mathbb{R}^r$,

$$A_a = \begin{bmatrix} 0 & 1 & 0 & \cdots & 0 & 0 \\ 0 & 0 & 1 & \cdots & 0 & 0 \\ 0 & 0 & 0 & \cdots & 0 & 0 \\ \vdots & \vdots & \vdots & \ddots & \vdots & \vdots \\ 0 & 0 & 0 & \cdots & 0 & 1 \\ -\sigma_0 & -\sigma_1 & -\sigma_2 & \cdots & -\sigma_{r-2} & -\sigma_{r-1} \end{bmatrix}, \tag{35}$$

$$B_a = [0, 0, \ldots, 0, 1]^T.$$

Because A_a is Hurwitz, e_a is bounded-input bounded output (BIBO) stable. With the convergence of s_1 to zero, e_0, e_1, …, e_{r-1} converge to zeros. Consequently, $e_r = -\sigma_0 e_0 - \sigma_1 e_1 - \cdots - \sigma_{r-1} e_{r-1}$ also converges to zero.

Step 3. With $z_2 = 0$,

$$s_2 = s_{2d}. \tag{36}$$

Because e_0, e_1, …, e_{r-1} converge to zeros and y_d has continuous derivatives up to the nth order, $\xi = -f_r(x_a) + y_d^{(r)} - d_1 - \sum_{i=1}^{r-1} \sigma_i e_{i+1}$ is bounded. Thus, a positive constant $\xi_{\max}$ exists such that $\xi_{\max} = \sup_t \xi(t)$. From (1), (18), and (36), we obtain

$$\begin{aligned} \dot{x}_{r+1} &= x_{r+2} \\ &\vdots \\ \dot{x}_{n-1} &= x_n \\ a_n x_n &= -\sum_{i=r+1}^{n-1} a_i x_i + \xi. \end{aligned} \tag{37}$$

Equation (37) is simplified as

$$\dot{x}_{b_z} = A_b x_{b_z} + B_b \xi \tag{38}$$

where $x_{b_z} = [x_{r+1}, x_{r+2}, \ldots, x_{n-1}]^T \in \mathbb{R}^{n-r-1}$,

$$A_b = \begin{bmatrix} 0 & 1 & 0 & \cdots & 0 & 0 \\ 0 & 0 & 1 & \cdots & 0 & 0 \\ 0 & 0 & 0 & \cdots & 0 & 0 \\ \vdots & \vdots & \vdots & \ddots & \vdots & \vdots \\ 0 & 0 & 0 & \cdots & 0 & 1 \\ -\frac{a_{r+1}}{a_n} & -\frac{a_{r+2}}{a_n} & -\frac{a_{r+3}}{a_n} & \cdots & -\frac{a_{n-2}}{a_n} & -\frac{a_{n-1}}{a_n} \end{bmatrix}, \tag{39}$$

$$B_b = \left[0, 0, \ldots, 0, \frac{1}{a_n}\right]^T.$$

We define the positive-definite Lyapunov function V_b as

$$V_b = x_{b_z}^T P_b x_{b_z}. \tag{40}$$

Because A_b is Hurwitz, a positive definite matrix P_b exists such that

$$A_b^T P_b + P_b A_b = -I. \tag{41}$$

The derivative of V_b is

$$\begin{aligned} \dot{V}_b &\le -x_{b_z}^T x_{b_z} + 2 x_{b_z}^T P_b B_b \xi_{\max} \\ &\le -\left\|x_{b_z}\right\|_2^2 + \frac{2\lambda_{\max}(P_b)\,\xi_{\max}}{a_n}\left\|x_{b_z}\right\|_2 \\ &\le -(1-\theta_1)\left\|x_{b_z}\right\|_2^2 - \theta_1\left\|x_{b_z}\right\|_2^2 \\ &\quad + \frac{2\lambda_{\max}(P_b)\,\xi_{\max}}{a_n}\left\|x_{b_z}\right\|_2 \end{aligned} \tag{42}$$

where $0 < \theta_1 < 1$, and $\lambda_{\min}(A)$ and $\lambda_{\max}(A)$ are the minimum and maximum eigenvalues of the matrix A, respectively. Then,

$$\dot{V}_b \le -(1-\theta_1)\left\|x_{b_z}\right\|_2^2 \tag{43}$$

for all $\|x_{b_z}\|_2 \le \mu_1$ where $\mu_1 = 2\lambda_{\max}(P_b)\xi_{\max}/\theta_1 a_n$. There exists T_1 such that

$$\left\|x_{b_z}\right\|_2 \le \frac{\lambda_{\max}(P_b)}{\lambda_{\min}(P_b)}\mu_1 \tag{44}$$

for all $t \ge T_1$. Consequently, x_b is also ultimately bounded with the ultimate bound of x_{b_z}. □

Remark 6. Owing to ξ in (38), only the boundedness of x_b is guaranteed. Furthermore, the convergence rate of x_b is fixed by the system parameters. Only the convergence of z_2 to z_{2_d} is sufficient to make e_1 converge to zero, regardless of the convergence rate of x_b.

Remark 7. When e_a converges to zero and $y_d(\infty)$ and d are zero, $\xi_{\max}$ becomes zero. Consequently, x_b also converges to zero.

Remark 8. In [22, 23], the coupled systems with multi-inputs were dealt; these techniques cannot solve the control problems for the coupled nonlinear system with single input (1). On the other hand, the proposed method (20) and (22) can solve the tracking control problems for the coupled nonlinear system with one input (1).

4. Closed-Loop Stability Analysis

Actually, controller (20) and (22) uses the estimated disturbances $\hat{d}_1$ and $\hat{d}_2$ instead of the disturbances d_1 and d_2. The controller becomes

$$s_{2d} = -f_r(x_a) + y_d^{(r)} - \hat{d}_1 - \sum_{i=0}^{r-1}\sigma_i e_{i+1} - k_{s1}s_1$$

$$u = -\frac{1}{a_n g(x)}\left(\sum_{i=r+1}^{n-1} a_i x_{i+1} - \dot{s}_{2d} + \phi_1(z_2) - \phi_2(z_2)\right) - \frac{1}{g(x)}\left(f_n(x) + \hat{d}_2\right) \tag{45}$$

where $\phi_1(z_2) = k_{z1}|z_2|^{1/2}\mathrm{sgn}(z_2)$, $\dot{\phi}_2(z_2) = -k_{z2}\,\mathrm{sgn}(z_2)$, and k_{s1}, k_{z1}, and k_z2 are positive constants. The closed-loop system including controller (45) and observer (4) is given as follows:

$$\begin{aligned}
\dot{s}_1 &= -k_{s1}s_1 + z_2 + \tilde{d}_1\\
\dot{z}_2 &= -k_{z1}|z_2|^{1/2}\,\mathrm{sgn}(z_2) + \phi_2 + \tilde{d}_2\\
\dot{\phi}_2 &= -k_{z2}\,\mathrm{sgn}(z_2)\\
\dot{\tilde{d}}_1 &= -\frac{1}{\varepsilon_1}\tilde{d}_1 + \dot{d}_1\\
\dot{\tilde{d}}_2 &= -\frac{1}{\varepsilon_2}\tilde{d}_2 + \dot{d}_2
\end{aligned} \tag{46}$$

Theorem 9. *With Assumptions 1 and 2, suppose that controller (45) and disturbance observer (7) and (8) are used in (1). Further, μ_{z_2} and T_{z_2} exist such that*

$$|z_2| \le \mu_{z_2} \tag{47}$$

for all $t \ge T_{z_2}$. The overall tracking error system (46) is the serial interconnected system of the ISS system. As $t \longrightarrow \infty$,

$$\begin{aligned}
|s_1(t)| &\le s_{1_{\max}}\\
|\tilde{d}_1(t)| &\le 2\varepsilon_1\dot{d}_{1_{\max}}\\
|\tilde{d}_2(t)| &\le 2\varepsilon_2\dot{d}_{2_{\max}}
\end{aligned} \tag{48}$$

where $s_{1_{\max}} = (2/k_{s1})(\mu_{z_2} + 2\varepsilon_1\dot{d}_{1_{\max}})$. Consequently, e_a and x_b are ultimately bounded.

Proof.
Step 1. In (46), the dynamics of z_2 and ϕ_2 are

$$\begin{aligned}
\dot{z}_2 &= -k_{z1}|z_2|^{1/2}\,\mathrm{sgn}(z_2) + \phi_2 + \tilde{d}_2\\
\dot{\phi}_2 &= -k_{z2}\mathrm{sgn}(z_2).
\end{aligned} \tag{49}$$

We define the vector $\zeta = [\zeta_1\ \ \zeta_2]^T = [|z_2|^{1/2}\mathrm{sgn}(z_2),\ \phi_2]^T$. The derivative of ζ with respect to time is

$$\dot{\zeta} = \frac{1}{|\zeta_1|}A_\zeta\zeta \tag{50}$$

where

$$A_\zeta = \begin{bmatrix} -\frac{1}{2}k_{z1} & \frac{1}{2}\\ -k_{z2} & 0\end{bmatrix} \tag{51}$$

and $|\zeta_1| = |z_2|^{1/2}$. Because $k_{z1} > 0$ and $k_{z2} > 0$, A_ζ is Hurwitz. We define the Lyapunov candidate function V_ζ as

$$V_\zeta = \zeta^T P_\zeta \zeta \tag{52}$$

where P_ζ is positive definite. The derivative of ζ with respect to time is given by

$$\dot{V}_\zeta = -\frac{1}{|\zeta_1|}\zeta^T Q_\zeta\zeta + \frac{1}{|\zeta_1|^{1/2}}\begin{bmatrix}\tilde{d}_2 & 0\end{bmatrix}P_\zeta\zeta \tag{53}$$

where Q_ζ is positive definite such that $A_\zeta^T P_\zeta + P_\zeta A_\zeta = -Q_\zeta$. From (10) and the definition of $V_{\tilde{d}_2} = \tilde{d}_2^2$, $\dot{V}_{\tilde{d}_2}$ is given by

$$\begin{aligned}
\dot{V}_{\tilde{d}_2} &= -\frac{1}{\varepsilon_2}\tilde{d}_2^2 + \dot{d}_2\tilde{d}_2 = -\frac{1}{\varepsilon_2}|\tilde{d}_2|^2 + \dot{d}2_{\max}|\tilde{d}_2|\\
&= -\left(\frac{1}{\varepsilon_2} - \theta_{\tilde{d}_2}\right)|\tilde{d}_2|^2 - \theta_{\tilde{d}_2}|\tilde{d}_2|^2 + \dot{d}2_{\max}|\tilde{d}_2|
\end{aligned} \tag{54}$$

where $0 < \theta_{\tilde{d}_2} < 1$. Then,

$$\dot{V}_{\tilde{d}_2} \le -\left(\frac{1}{\varepsilon_2} - \theta_{\tilde{d}_2}\right)|\tilde{d}_2|^2 \tag{55}$$

for all $|\tilde{d}_2| \ge \mu_{\tilde{d}_2}$ where $\mu_{\tilde{d}_2} = \dot{d}2_{\max}/\theta_{\tilde{d}_2}$. There exists $T_{\tilde{d}_2}$ such that

$$|\tilde{d}_2| \le \mu_{\tilde{d}_2} \tag{56}$$

for all $t \ge T_{\tilde{d}_2}$ When $t \ge T_{\tilde{d}_2}$, (53) becomes

$$\begin{aligned}
\dot{V}_\zeta &\le -\frac{1}{|\zeta_1|}\left(\zeta^T Q_\zeta\zeta + \mu_{\tilde{d}_2}\lambda(P_\zeta)\|\zeta\|_2\right)\\
&\le \frac{1}{|\zeta_1|}\left(-\left(\lambda_{\min}(Q_\zeta) - \theta_\zeta\right)\|\zeta\|^2 - \theta_\zeta\|\zeta\|^2 + \mu_{\tilde{d}_2}\lambda(P_\zeta)\|\zeta\|_2\right)
\end{aligned} \tag{57}$$

where $0 < \theta_\zeta < 1$. Then,

$$\dot{V}_\zeta \le \frac{1}{|\zeta_1|}\left(-\left(\lambda_{\min}(Q_\zeta) - \theta_\zeta\right)\|\zeta\|^2\right) \tag{58}$$

for all $\|\zeta\|_2 \ge \mu_\zeta$ where $\mu_\zeta = \mu_{\tilde{d}_2}\lambda(P_\zeta)/\theta_\zeta$. There exists T_ζ such that

$$\|\zeta\|_2 \le \frac{\lambda_{\max}(P_\zeta)}{\lambda_{\min}(P_\zeta)}\mu_\zeta \tag{59}$$

for all $t \ge T_\zeta$. Consequently, μ_{z_2} and T_{z_2} exist such that

$$|z_2| \le \mu_{z_2} \tag{60}$$

for all $t \geq T_{z_2}$. In (46), s_1 dynamics can be obtained as

$$\dot{s}_1 = -k_{s1} s_1 + z_2 + \tilde{d}_1. \tag{61}$$

Then we obtain the dynamics of s_1^2 as

$$\begin{aligned} \frac{d}{dt}\left(\frac{s_1^2}{2}\right) &= -k_{s1} s_1^2 + s_1\left(z_2 + \tilde{d}_1\right) \\ &\leq -\frac{k_{s1}}{2} s_1^2 \\ &\quad - \frac{k_{s1}}{2}\left|s_1\right|\left(\left|s_1\right| - \frac{2}{k_{s1}}\left(\left|z_2\right| + \left|\tilde{d}_1\right|\right)\right). \end{aligned} \tag{62}$$

From (62), the following result is derived using Lemma 6.20 and Theorem C.2 in [11]:

$$\begin{aligned} \left|s_1(t)\right| &\leq \exp\left(-\frac{k_{s1}}{2} t\right)\left|s_1(0)\right| \\ &\quad + \frac{2}{k_{s1}} \sup_{0 \leq \tau \leq t}\left(\left|z_2(\tau)\right| + \left|\tilde{d}_1(\tau)\right|\right). \end{aligned} \tag{63}$$

Equation (63) shows that the relationship between z_2 and $\tilde{d}_1$, and e_{i+1} has ISS property. The overall tracking error system (46) is the serial interconnected system of the ISS system. As $t \longrightarrow \infty$,

$$\begin{aligned} \left|s_1(t)\right| &\leq s_{1_{\max}} \\ \left|\tilde{d}_1(t)\right| &\leq 2\varepsilon_1 \dot{d}_{1_{\max}} \\ \left|\tilde{d}_2(t)\right| &\leq 2\varepsilon_2 \dot{d}_{2_{\max}} \end{aligned} \tag{64}$$

where $s_{1_{\max}} = (2/k_{s1})(\mu_{z_2} + 2\varepsilon_1 \dot{d}_{1_{\max}})$.

Step 2. Equation (16) can be rewritten as

$$\begin{aligned} \dot{e}_0 &= e_1 \\ &\vdots \\ \dot{e}_{r-1} &= e_r \\ e_r &= -\sum_{i=0}^{r-1} \sigma_i e_i + s_1. \end{aligned} \tag{65}$$

Equation (65) is simplified as

$$\dot{e}_a = A_a e_a + B_a s_1 \tag{66}$$

where $e_a = [e_0, e_1, \ldots, e_{r-1}]^T \in \mathbb{R}^r$,

$$A_a = \begin{bmatrix} 0 & 1 & 0 & \cdots & 0 & 0 \\ 0 & 0 & 1 & \cdots & 0 & 0 \\ 0 & 0 & 0 & \cdots & 0 & 0 \\ \vdots & \vdots & \vdots & \ddots & \vdots & \vdots \\ 0 & 0 & 0 & \cdots & 0 & 1 \\ -\sigma_0 & -\sigma_1 & -\sigma_2 & \cdots & -\sigma_{r-2} & -\sigma_{r-1} \end{bmatrix}, \tag{67}$$

$$B_a = [0, 0, \ldots, 0, 1]^T.$$

Because A_a is Hurwitz, e_a is BIBO stable. In (63) it was shown that s_1 is ultimately bounded and that $|s_1(t)| \leq s_{1_{\max}}$ as $t \longrightarrow \infty$. Thus, as $t \longrightarrow \infty$, (66) can be rewritten as follows:

$$\dot{e}_a \leq A_a e_a + B_a s_{1_{\max}} \tag{68}$$

We define the positive-definite Lyapunov function V_a as

$$V_a = e_a^T P_a e_a. \tag{69}$$

Because A_a is Hurwitz, a positive definite matrix P_a exists such that

$$A_a^T P_a + P_a A_a = -I. \tag{70}$$

The derivative of V_a is

$$\begin{aligned} \dot{V}_a &\leq -e_a^T e_a + 2 e_a^T P_a B_a s_{1_{\max}} \\ &\leq -\left\|e_a\right\|_2^2 + 2\lambda_{\max}(P_a)\, s_{1_{\max}} \left\|e_a\right\|_2 \\ &\leq -(1-\theta_e)\left\|e_a\right\|_2^2 - \theta_e \left\|e_a\right\|_2^2 \\ &\quad + 2\lambda_{\max}(P_a)\, s_{1_{\max}} \left\|e_a\right\|_2. \end{aligned} \tag{71}$$

Then,

$$\dot{V}_a \leq -(1-\theta_e)\left\|e_a\right\|_2^2 \tag{72}$$

for all $\|e_a\|_2 \leq \mu_1$ where $\mu_e = 2\lambda_{\max}(P_a) s_{1_{\max}}/\theta_e$. Consequently, e_a converges to the bounded ball, B_{e_a} as

$$B_{e_a} = \left\{ e_a \mid \left\|e_a\right\|_2 \leq \frac{\lambda_{\max}(P_a)}{\lambda_{\min}(P_a)} \mu_e \right\} \tag{73}$$

as $t \longrightarrow \infty$.

Step 3. With $|z_2| \leq \mu_{z_2}$, we obtain

$$\begin{aligned} \dot{x}_{r+1} &= x_{r+2} \\ &\vdots \\ \dot{x}_{n-1} &= x_n \\ a_n x_n &\leq -\sum_{i=r+1}^{n-1} a_i x_i + \xi + \mu_{z_2}. \end{aligned} \tag{74}$$

Because $e_0, e_1, \ldots, e_{r-1}$ converge to the bounded ball B_a and because y_d has continuous derivatives up to the nth order, $\xi = -f_r(x_a) + y_d^{(r)} - d_1 - \sum_{i=1}^{r-1} \sigma_i e_{i+1}$ is bounded. Equation (74) is simplified as

$$\dot{x}_{b_z} \leq A_b x_{b_z} + B_b\left(\xi_{\max} + \mu_{z_2}\right). \tag{75}$$

We define the positive-definite Lyapunov function V_b as

$$V_b = x_{b_z}^T P_b x_{b_z}. \tag{76}$$

Because A_b is Hurwitz, a positive definite matrix P_b exists such that

$$A_b^T P_b + P_b A_b = -I. \tag{77}$$

The derivative of V_b is

$$\begin{aligned}\dot{V}_b &\le -x_{b_z}^T x_{b_z} + 2x_b^T P_b B_b \left(\xi_{\max} + \mu_{z_2}\right) \\ &\le -\left\|x_{b_z}\right\|_2^2 + \frac{2}{a_n}\lambda_{\max}\left(P_b\right)\left(\xi_{\max} + \mu_{z_2}\right)\left\|x_{b_z}\right\|_2 \\ &\le -\left(1-\theta_2\right)\left\|x_{b_z}\right\|_2^2 - \theta_2\left\|x_{b_z}\right\|_2^2 \\ &\quad + \frac{2\lambda_{\max}\left(P_b\right)}{a_n}\left(\xi_{\max} + \mu_{z_2}\right)\left\|x_{b_z}\right\|_2.\end{aligned} \tag{78}$$

where $0 < \theta_2 < 1$. Then,

$$\dot{V}_b \le -\left(1-\theta_1\right)\left\|x_{b_z}\right\|_2^2 \tag{79}$$

for all $\|x_{b_z}\|_2 \le \mu_2$ where $\mu_2 = (2\lambda_{\max}(P_b)/\theta_2 a_n)(\xi_{\max} + \mu_{z_2})$. From Theorem 4.18 of [9], there exists T_2 such that

$$\left\|x_{b_z}\right\|_2 \le \frac{\lambda_{\max}\left(P_b\right)}{\lambda_{\min}\left(P_b\right)}\mu_2 \tag{80}$$

for all $t \ge T_2$. Consequently, x_b is also ultimately bounded with the ultimate bound of x_{b_z}. □

Remark 10. As the controller gains k_1 and k_2, and the observer gains $1/\varepsilon_1$ and $1/\varepsilon_2$ increase, $\|e_a\|_2$ becomes smaller. If the disturbances d_1 and d_2 are constant, we see that the disturbance estimation errors $\tilde{d}_1$ and $\tilde{d}_2$ converge to zeros from (12). Then, e_a converges to zero. Consequently, the output tracking error e_1 converges to zero.

5. Performance Analysis

5.1. Numerical Simulation Study. Simulations were performed to analyze the performance of the proposed method. In these simulations, we used the system

$$\begin{aligned}\dot{x}_1 &= x_2 \\ \dot{x}_2 &= 3x_1x_2 + \sin\left(x_2\right) + 20x_3 + 4x_4 + d_1 \\ \dot{x}_3 &= x_4 \\ \dot{x}_4 &= x_1^2 + 2x_2 + 3\sin\left(2x_3\right) + x_4 \\ &\quad + \left(1 + 0.5\cos\left(0.1x_1\right)\right)u + d_2\end{aligned} \tag{81}$$

where $d_1 = \sin(\pi t)$ and $d_2 = 2 + \cos(5x_1)$. The desired reference trajectory $x_{1_d} = (1 - e^{-2t})\sin(0.2t)$ was used. The controller was designed as

$$\begin{aligned}\xi_1 &= \hat{d}_1 - \frac{x_2}{\varepsilon_1} \\ \xi_2 &= \hat{d}_2 - \frac{x_4}{\varepsilon_2} \\ \dot{\xi}_1 &= -\frac{1}{\varepsilon_1}\left(\xi_1 + \frac{x_r}{\varepsilon_1}\right) + \frac{1}{\varepsilon_1}\left(-3x_1x_2 - \sin\left(x_2\right) - 2x_3\right. \\ &\quad \left. - 4x_4\right) \\ \dot{\xi}_2 &= -\frac{1}{\varepsilon_2}\left(\xi_2 + \frac{x_n}{\varepsilon_2}\right) - \frac{1}{\varepsilon_2}\left(-x_1^2 - 2x_2 - 3\sin\left(2x_3\right)\right. \\ &\quad \left. - x_4\right) + \frac{1}{\varepsilon_2}\left(1 + 0.5\cos\left(0.1x_1\right)\right)u \\ s_1 &= \sigma_0 e_0 + \sigma_1 e_1 + e_2 \\ s_2 &= 2x_3 + 4x_4 \\ s_{2d} &= -\left(3x_1x_2 + \sin\left(x_2\right)\right) + \ddot{y}_d - \hat{d}_1 - \left(\sigma_0 e_1 + \sigma_1 e_2\right) \\ &\quad - k_{s1}s_1 \\ u &= -\frac{1}{4\left(1 + 0.5\cos\left(0.1x_1\right)\right)}\left(a_3x_4 - \dot{s}_{2d} + \phi_1\left(z_2\right)\right. \\ &\quad \left. - \phi_2\left(z_2\right)\right) - \frac{1}{\left(1 + 0.5\cos\left(0.1x_1\right)\right)}\left(x_1^2 + 2x_2\right. \\ &\quad \left. + 3\sin\left(2x_3\right) + x_4 + \hat{d}_2\right)\end{aligned} \tag{82}$$

where $\phi_1(z_2) = k_{z1}|z_2|^{1/2}\mathrm{sgn}(z_2)$ and $\dot{\phi}_2(z_2) = -k_{z2}\,\mathrm{sgn}(z_2)$. In controller (82), the following parameters were used: $k_{s1} = 1000$, $k_{z1} = 20$, $k_{z2} = 10$, $\sigma_0 = 100$, $\sigma_1 = 20$, $\varepsilon_1 = 0.1$, and $\varepsilon_2 = 0.05$.

The estimation performance of the DOB is shown in Figure 1. The disturbances were well estimated by the DOB. The tracking performances of s_1 and s_2 are shown in Figure 2. s_1 and s_2 converged to the neighborhood of zero and neighborhood of s_{2_d}, respectively, because the controller and observer gains were sufficiently high to suppress the effect of the estimation error. The tracking performance and state variables are shown in Figures 3 and 4. We see that both tracking errors e_1 and e_2 converged to almost zero because of the proposed controller (82). Because of the disturbance and nonzero trajectory, state variables x_3 and x_4 did not converge to zeros, but were bounded. Figure 5 shows the control input. Because the control method was designed using STA, there was no chattering problem.

5.2. Application to Differential Braking Control in Vehicle Lateral Dynamics. To evaluate the performance of the proposed method in a practical system, the proposed method was applied to the differential braking control system in a vehicle. In the vehicular control system, the lateral position is controlled for avoiding collisions using differential brake forces when the driver changes the lane under collision risk or with a vehicle in the blind spot [25]. The lateral control system with the differential braking is

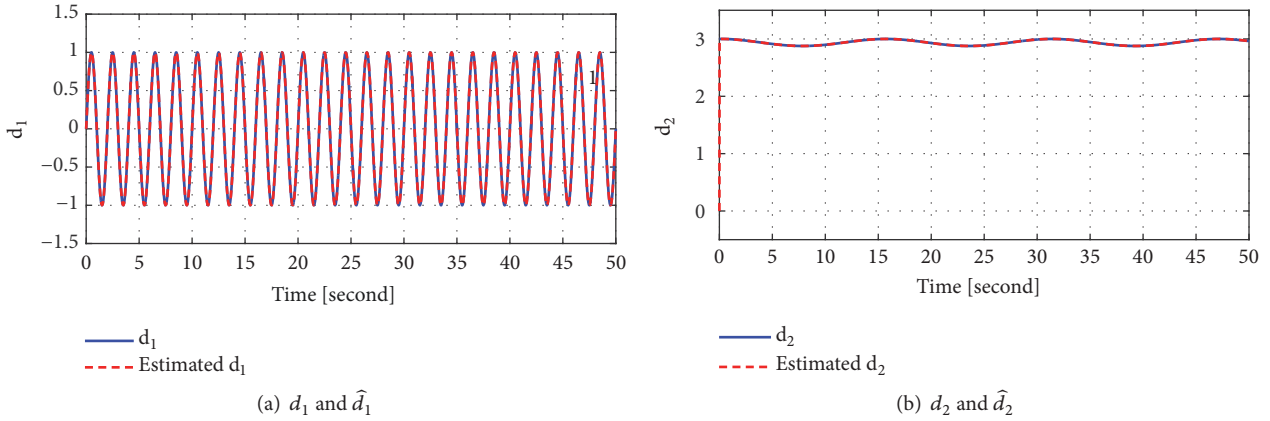

(a) d_1 and $\hat{d}_1$ (b) d_2 and $\hat{d}_2$

Figure 1: Estimated disturbances.

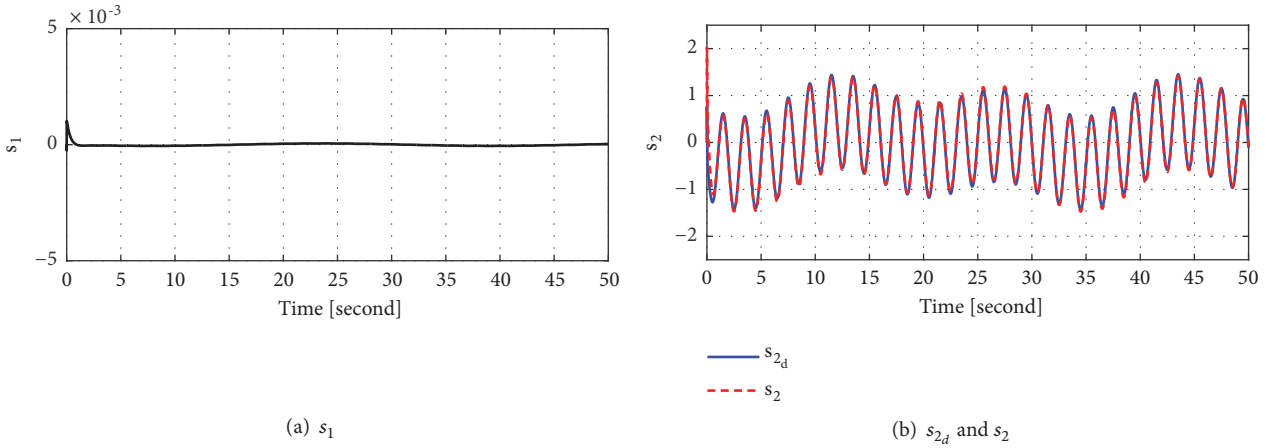

(a) s_1 (b) s_{2_d} and s_2

Figure 2: Tracking performances of s_1 and s_2.

$$\begin{aligned}
\dot{e}_1 &= e_2 \\
\dot{e}_2 &= a_{22}e_2 + a_{23}e_3 + a_{24}e_4 + b_{\delta 2}\delta + b_{w2}\dot{\psi}_d + d_1 \\
\dot{e}_3 &= e_4 \\
\dot{e}_4 &= a_{42}e_2 + a_{43}e_3 + a_{44}e_4 + b_{\delta 4}\delta + b_{w4}\dot{\psi}_d + b_{F4}F_{bs} \\
&\quad + d_2.
\end{aligned} \tag{83}$$

where e_1 is the lateral offset, e_2 is the derivative of the lateral offset, e_3 is the yaw error, e_4 is the yaw error rate, F_{bs} is the differential braking force control input, δ is the steering wheel angle, $\dot{\psi}_d$ is the desired yaw rate, d_1 is the disturbance including the driver torque and modeling error, and d_2 is the disturbance including self-aligned torque, modeling error, etc. The detailed definitions of the parameters can be found in [28]. The aim of controller design is to determine the brake steer force F_{bs} that makes

$$\lim_{t\longrightarrow\infty} e_1(t) = 0. \tag{84}$$

when the driver attempts the lane change under a collision risk or with a vehicle in the blind spot. This system (83) satisfies Assumption 2. The controller is designed as

$$\begin{aligned}
\xi_1 &= \hat{d}_1 - \frac{x_r}{\varepsilon_1} \\
\xi_2 &= \hat{d}_2 - \frac{x_n}{\varepsilon_2} \\
\dot{\tilde{\xi}}_1 &= -\frac{1}{\varepsilon_1}\left(\xi_1 + \frac{x_r}{\varepsilon_1}\right) + \frac{1}{\varepsilon_1}\left(-a_{22}e_2 - a_{23}e_3 - a_{24}e_4 -\right) \\
\dot{\tilde{\xi}}_2 &= -\frac{1}{\varepsilon_2}\left(\xi_2 + \frac{x_n}{\varepsilon_2}\right) + \frac{1}{\varepsilon_2}\left(-a_{42}e_2 - a_{43}e_3 - a_{44}e_4\right. \\
&\quad \left. - b_{F4}F_{bs}\right) \\
s_1 &= \sigma_0 e_0 + \sigma_1 e_1 + e_2 \\
s_2 &= a_{23}e_3 + a_{24}e_4 \\
s_{2d} &= -\sigma_0 e_1 - \sigma_1 e_2 - a_{22}e_2 - b_{\delta 2}\delta - b_{w2}\dot{\psi}_d - d_1 \\
&\quad - k_{s1}s_1 \\
F_{bs} &= -\frac{1}{a_{24}b_{F4}}\left[a_{23}e_4\right. \\
&\quad \left. + a_{24}\left(a_{42}e_2 + a_{43}e_3 + a_{44}e_4 + d_2\right)\right]
\end{aligned}$$

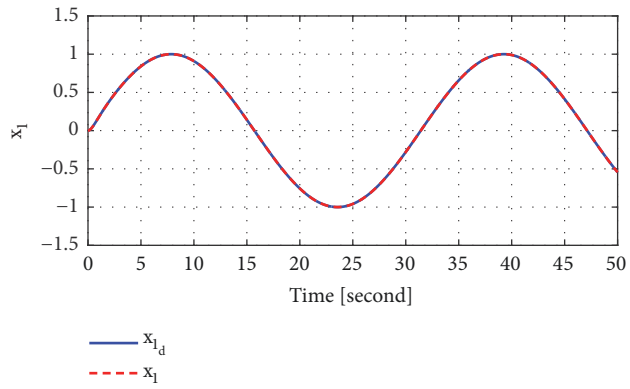

(a) x_{1_d} and x_1

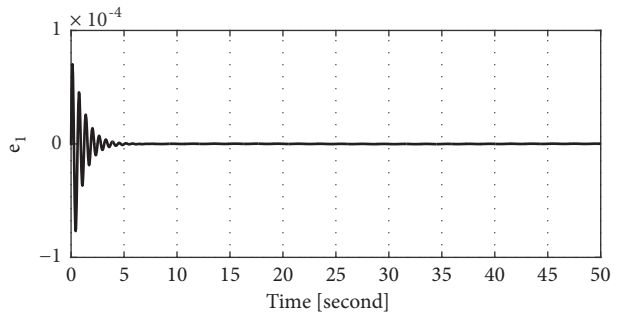

(b) e_1

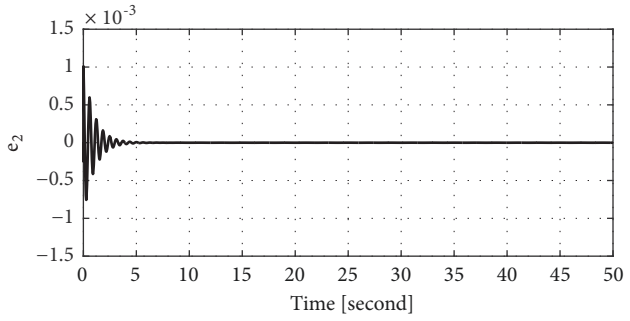

(c) e_2

FIGURE 3: x_1 tracking performance and errors.

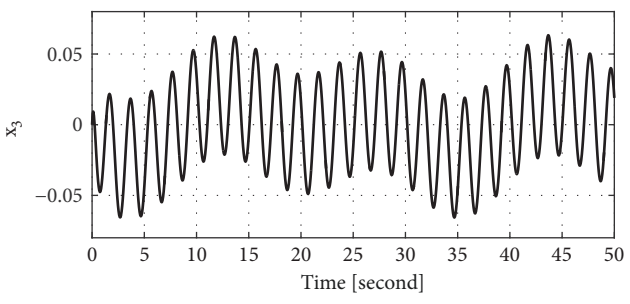

(a) x_3

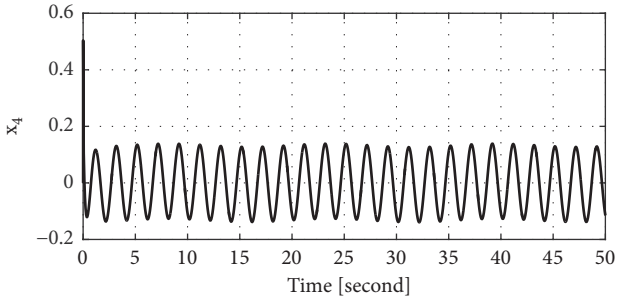

(b) x_4

FIGURE 4: x_3 and x_4.

$$-\frac{1}{a_{24}b_{F4}}\left[a_{24}\left(b_{\delta 4}\delta + b_{w4}\dot{\psi}_d\right) - \dot{s}_{2d} + \phi_1\left(z_2\right) - \phi_2\left(z_2\right)\right] \tag{85}$$

where $\phi_1(z_2) = k_{z1}|z_2|^{1/2}\text{sgn}(z_2)$ and $\dot{\phi}_2(z_2) = -k_{z2}\,\text{sgn}(z_2)$, $\sigma_0 = 1000000$, $\sigma_1 = 200$, $\sigma_3 = 50$, $\sigma_4 = 0$, $k_{s1} = 5$, $k_{z1} = 1$, $k_{z2} = 0.1$, $\varepsilon_1 = 0.5$, and $\varepsilon_2 = 0.5$. The velocity of the vehicle is 80 km/h on a straight road. The test scenario is as follows: (1) at 5 sec., the driver attempts lane change under collision risk with the object vehicle in the target lane; (2) as soon as the driver attempts lane change, the differential braking control (DBC) system is activated with a warning against the collision risk; (3) the driver attempts to keep the original lane with the help of the DBC; (4) the DBC system operates to move the vehicle to the center of the original lane.

Simulations were performed using the vehicle dynamic software CarSim and Matlab/Simulink as shown in Figure 6. The S-function coded in C language was used for implementing the proposed sliding mode backstepping control method. The output of CarSim consists of vehicle motion data such as steer angle, lateral velocity, and brake force. We also modeled the lane camera sensor to obtain the lane coefficients [29]; c_0 denotes the lateral lane center offset at c.g., c_1 denotes the in-lane heading slop, the heading angle error at c.g., c_2 denotes

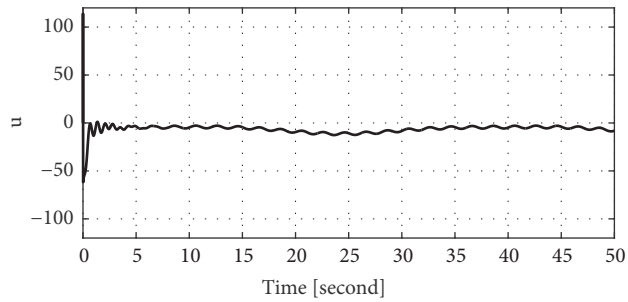

Figure 5: Control input.

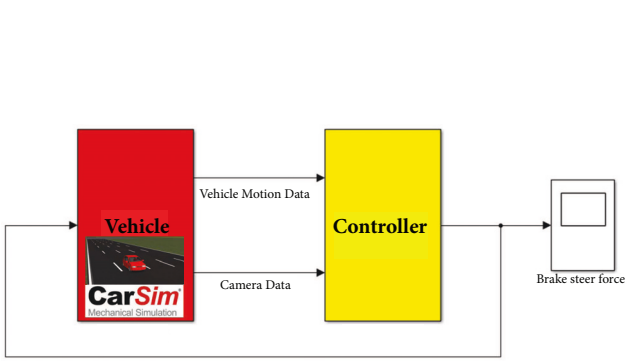

(a) Overall simulation structure that consists of CarSim vehicle model

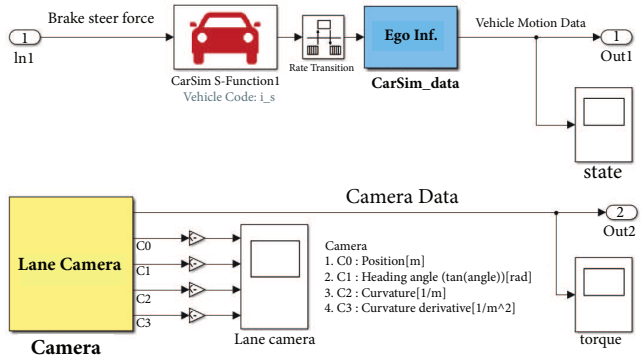

(b) Vehicle part. The output of lane camera is lane coefficients; c_0 denotes the lateral lane center offset at c.g., c_1 denotes the in-lane heading slop, the heading angle error at c.g., c_2 denotes curvature/2 at $s = 0$, and c_3 denotes the curvature-rate/6

Figure 6: Vehicle and camera models used in the simulations.

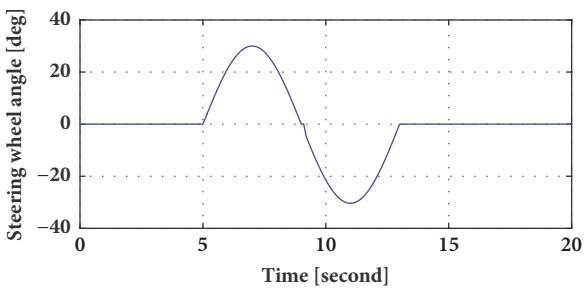

Figure 7: Steering wheel angle.

curvature/2 at $s = 0$, and c_3 denotes the curvature-rate/6. The steering wheel angle used in the simulations is shown in Figure 7.

Two cases were tested: (1) driving with proposed controller (85); (2) driving without proposed controller (85). The simulation results are shown in Figure 8. The lateral offset errors of the two cases are depicted in Figure 8(a). Figure 8(b) shows the control input. Because the control method was designed using STA, there was no chattering problem. In case 2 (without DBC), for the given steering wheel angle, the lateral offset error e_1 becomes 1.1 m owing to the steering wheel angle. On the other hand, in case 1 (with DBC), the lateral offset error e_1 was maintained to nearly zero because the brake steer force compensated for the steering wheel angle using the proposed method (85). The yaw rate error e_4 was also kept to nearly zero. Figure 9 shows the estimated disturbance. External disturbances appeared owing to the bank angle, road reaction force, the assumptions for this modeling, etc. The external disturbances were compensated by using utilizing the proposed method. Consequently, the lateral offset e_1 converged to zero despite the steer angle and the disturbances.

6. Conclusions

In this paper, we proposed a sliding-mode backstepping control for the coupled normal form of nonlinear systems. The proposed method was developed by combining backstepping and sliding-mode control. The key idea of the proposed method is that the linear terms of the state variables of the second subsystem are lumped into the virtual input in the first subsystem. To compensate for the disturbances, a DOB was developed. The stability of the closed-loop is validated by using the ISS property. Through numerical simulations and application to a vehicle system, the proposed method was observed to lead to convergence of the output to the desired output trajectory under the described disturbances.

The main drawback is the use of the derivative of the measured signal in the controller. It may result in the

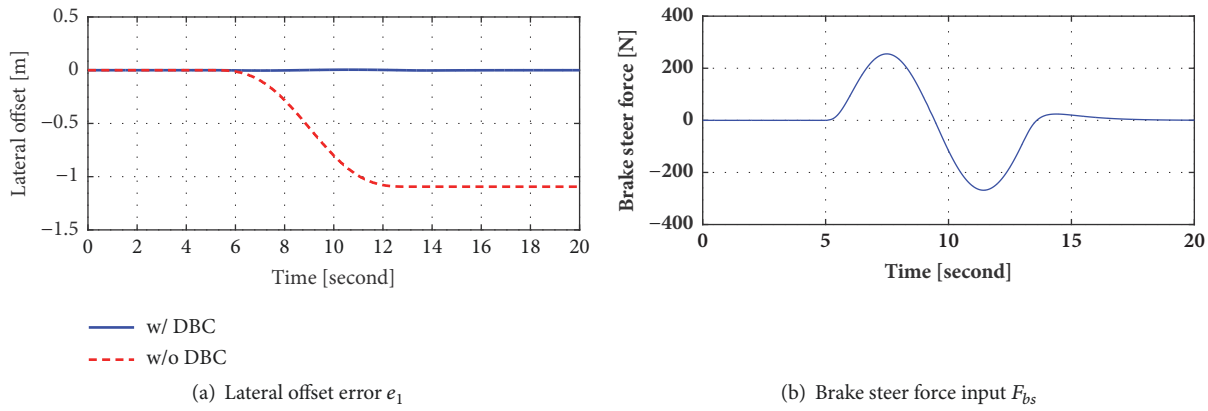

(a) Lateral offset error e_1 (b) Brake steer force input F_{bs}

Figure 8: Control performance.

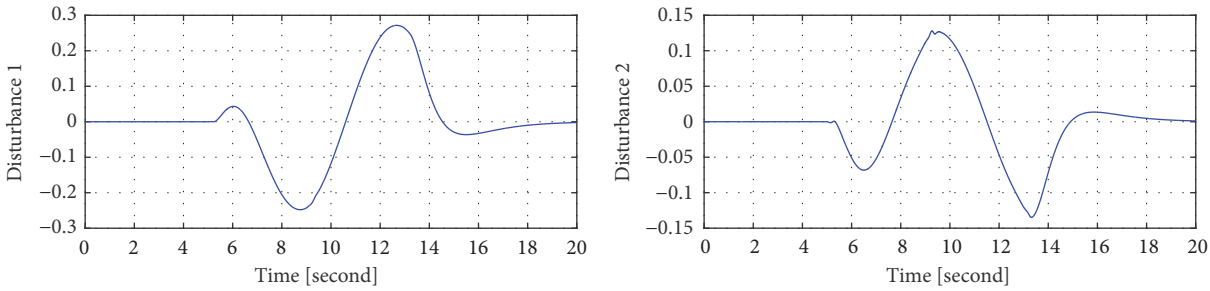

(a) d_1 (b) d_2

Figure 9: Estimated disturbances.

amplification of the measurement noise. Generally, the filter technique is widely used to obtain the derivatives of the measured signals without the amplification of the measurement noise [30, 31]. However, the use of the filter may cause the phase lag in the feedback loop. In future works, we will develop the control method with the consideration of the amplification of the measurement noise in the derivatives of the measured signals.

Data Availability

The data used to support the findings of this study are included within the article.

Conflicts of Interest

The authors declare that they have no conflicts of interest.

Acknowledgments

This research was supported by the Basic Science Research Program through the National Research Foundation of Korea funded by the Ministry of Education under Grant NRF-2016R1C1B1014831 and the Research Program, Development of High Voltage Brake System for Response to Safety Regulations of Micro eMobility (20003066), funded by the Ministry of Trade, Industry and Energy (MOTIE, Korea).

References

[1] R. A. Freeman and J. A. Primbs, "Control Lyapunov new ideas from an functions: old source," in *Proceedings of the 35th IEEE Conference on Decision and Control*, pp. 3926–3931, December 1996.

[2] X. Huang, W. Lin, and B. Yang, "Global finite-time stabilization of a class of uncertain nonlinear systems," *Automatica*, vol. 41, no. 5, pp. 881–888, 2005.

[3] W. M. Haddad and V. Chellaboina, *Nonlinear Dynamical Systems and Control. A Lyapunov-Based Approach*, Princeton University Press, Princeton, NJ, USA, 2008.

[4] W. Kim, D. Shin, and C. C. Chung, "The Lyapunov-based controller with a passive nonlinear observer to improve position tracking performance of microstepping in permanent magnet stepper motors," *Automatica*, vol. 48, no. 12, pp. 3064–3074, 2012.

[5] A. Isidori, *Nonlinear Control Systems: An Introduction*, Springer, Berlin, Germany, 2nd edition, 1989.

[6] C. Xia, Q. Geng, X. Gu, T. Shi, and Z. Song, "Input, output feedback linearization and speed control of a surface permanent-magnet synchronous wind generator with the boost-chopper

converter," *IEEE Transactions on Industrial Electronics*, vol. 59, no. 9, pp. 3489–3500, 2012.

[7] V. Utkin, J. Guldner, and J. Shi, *Sliding Mode Control in Electromechanical Systems*, Taylor & Franci, Philadelphia, PA, USA, 1999.

[8] C. Guan and S. Pan, "Adaptive sliding mode control of electro-hydraulic system with nonlinear unknown parameters," *Control Engineering Practice*, vol. 16, no. 11, pp. 1275–1284, 2008.

[9] H. Khalil, *Nonlinear Systems*, Prentice-Hall, Upper Saddle River, NJ, USA, 3rd edition, 2002.

[10] W. Kim, D. Shin, Y. Lee, and C. C. Chung, "Simplified torque modulated microstepping for position control of permanent magnet stepper motors," *Mechatronics*, vol. 35, pp. 162–172, 2016.

[11] M. Krstić, I. Kanellakopoulos, and P. Kokotovic', *Nonlinear and Adaptive Control Design*, Wiley, New York, NY, USA, 1995.

[12] A. Alleyne and R. Liu, "A simplified approach to force control for electro-hydraulic systems," *Control Engineering Practice*, vol. 8, no. 12, pp. 1347–1356, 2000.

[13] J. Zhou, C. Wen, and Y. Zhang, "Adaptive backstepping control of a class of uncertain nonlinear systems with unknown backlash-like hysteresis," *IEEE Transactions on Automatic Control*, vol. 49, no. 10, pp. 1751–1757, 2004.

[14] J. J. Choi, S. I. Han, and J. S. Kim, "Development of a novel dynamic friction model and precise tracking control using adaptive back-stepping sliding mode controller," *Mechatronics*, vol. 16, no. 2, pp. 97–104, 2006.

[15] J. Yao, Z. Jiao, and D. Ma, "Extended-state-observer-based output feedback nonlinear robust control of hydraulic systems with backstepping," *IEEE Transactions on Industrial Electronics*, vol. 61, no. 11, pp. 6285–6293, 2014.

[16] S.-I. Han and J.-M. Lee, "Recurrent fuzzy neural network backstepping control for the prescribed output tracking performance of nonlinear dynamic systems," *ISA Transactions®*, vol. 53, no. 1, pp. 33–43, 2014.

[17] J. Yao, Z. Jiao, and D. Ma, "Adaptive robust control of dc motors with extended state observer," *IEEE Transactions on Industrial Electronics*, vol. 61, no. 7, pp. 3630–3637, 2014.

[18] W. Kim and C. C. Chung, "Robust output feedback control for unknown non-linear systems with external disturbance," *IET Control Theory & Applications*, vol. 10, no. 2, pp. 173–182, 2016.

[19] J. Yao and W. Deng, "Active disturbance rejection adaptive control of uncertain nonlinear systems: theory and application," *Nonlinear Dynamics*, vol. 89, no. 3, pp. 1611–1624, 2017.

[20] J. Yao and W. Deng, "Active disturbance rejection adaptive control of hydraulic servo systems," *IEEE Transactions on Industrial Electronics*, vol. 64, no. 10, pp. 8023–8032, 2017.

[21] C. M. Kang, W. Kim, and C. C. Chung, "Observer-based backstepping control method using reduced lateral dynamics for autonomous lane-keeping system," *ISA Transactions®*, vol. 83, pp. 214–226, 2018.

[22] S. Bouabdallah and R. Siegwart, "Backstepping and sliding-mode techniques applied to an indoor micro quadrotor," in *Proceedings of the IEEE International Conference on Robotics and Automation*, pp. 2247–2252, Barcelona, Spain, April 2005.

[23] H. Y. Li and Y. A. Hu, "Robust sliding-mode backstepping design for synchronization control of cross-strict feedback hyperchaotic systems with unmatched uncertainties," *Communications in Nonlinear Science and Numerical Simulation*, vol. 16, no. 10, pp. 3904–3913, 2011.

[24] W.-H. Chen, D. J. Ballance, P. J. Gawthrop, and J. O'Reilly, "A nonlinear disturbance observer for robotic manipulators," *IEEE Transactions on Industrial Electronics*, vol. 47, no. 4, pp. 932–938, 2000.

[25] R. Rajamani, *Vehicle Dynamics and Control*, Springer, New York, NY, USA, 2nd edition, 2012.

[26] A. Levant, "Sliding order and sliding accuracy in sliding mode control," *International Journal of Control*, vol. 58, no. 6, pp. 1247–1263, 1993.

[27] J. A. Moreno and M. Osorio, "Strict Lyapunov functions for the super-twisting algorithm," *IEEE Transactions on Automatic Control*, vol. 57, no. 4, pp. 1035–1040, 2012.

[28] Y. S. Son, W. Kim, S.-H. Lee, and C. C. Chung, "Robust multirate control scheme with predictive virtual lanes for lane-keeping system of autonomous highway driving," *IEEE Transactions on Vehicular Technology*, vol. 64, no. 8, pp. 3378–3391, 2015.

[29] C. M. Kang, S. Lee, and C. C. Chung, "Comparative evaluation of dynamic and kinematic vehicle models," in *Proceedings of the IEEE 53rd Annual Conference on Decision and Control (CDC '14)*, pp. 648–653, Los Angeles, Calif, USA, December 2014.

[30] B. Kristiansson and B. Lennartson, "Robust tuning of PI and PID controllers: using derivative action despite sensor noise," *IEEE Control Systems Magazine*, vol. 26, no. 1, pp. 55–69, 2006.

[31] J. Q. Han, "From PID to active disturbance rejection control," *IEEE Transactions on Industrial Electronics*, vol. 56, no. 3, pp. 900–906, 2009.